# Efficient Numerical Algorithm for Cascaded Raman Fiber Lasers Using a Spectral Method

Hakan I. Tarman and Halil Berberoğlu

***Abstract*—Over recent decades, fiber Raman lasers (FRLs) have received much attention from researchers and have become a challenge for them both numerically and experimentally. The equations governing the FRLs are in the form of a first-order system of nonlinear two-point boundary-value ordinary differential equations. In this paper, an algorithm for solving this system of differential equations using a spectral method, namely Chebyshev pseudospectral method, is presented in detail and then numerical simulations are performed. The main advantage of the spectral methods is in their optimality in achieving high accuracy by using fewer degrees of freedom under suitable conditions. It is shown that the proposed spectral method in combination with the Newton method results in a considerable reduction in the size of the discretized problem and in the computational effort to achieve high accuracy. In this paper, a new approach for constructing an initial approximate solution for the Newton iteration is also presented.**

***Index Terms*—Boundary-value problems (BVPs), fiber Raman lasers (FRLs), spectral method.**

## I. Introduction

ALTHOUGH the nonlinearity may not always be desired in photonic applications, it becomes useful in some fields such as multiwavelength fiber Raman lasers (FRLs). Much of the interest in FRLs stem from their ability to be compatible with optical fiber communication systems and their becoming a key technology in versatile applications such as pump sources for Raman and rare-earth fiber amplifiers, spectroscopy, etc. FRLs are based on a well-known nonlinear optical process called stimulated Raman scattering (SRS) [1], [2] where the incident pump photon generates the next Stokes light, thus resulting in a frequency down-shifted Stokes light in cascading processes. The first classical description of the theory of cw Raman oscillation in optical fibers were presented in [3].

The processes are described by a first-order system of nonlinear two-point boundary-value ordinary differential equations with boundary conditions relating to the reflection coefficients of the mirrors at each end of the fiber laser. The model equations govern the power distributions along the fiber. They have been tested with experiments [4], [5] and the agreement between theory and experiment is shown to be very good. Besides prediction, optimization of the output power of the laser to achieve maximum efficiency is shown to be an important design problem [6], [7]. For this purpose the model equations are to be solved to determine the effects of different parameters of the laser on the efficiency. Due to the nonlinearity, coupled with the boundary conditions representing the reflected laser power by Bragg gratings, the general approach to this system is numerical and it is quite a challenging one. Only with varying degree of simplifying approximations, an analytical solution may be possible [8]–[10]. For prediction purposes or for the task of optimization that requires repeated computations, an efficient and robust numerical solution method is particularly important.

Most numerical approaches in literature employ local approximations for the dependent variables with their derivatives to reduce the model differential equations to a system of nonlinear algebraic equations. These approximations may be in the form of finite differences or spline interpolation over a collocation grid [11], [6]. Some of these are applied within boundary-value problem (BVP) solver package programs, such as COLSYS [12] or bvp4c [13]. Initial value problem (IVP) solvers, such as Runge–Kutta methods are also widely employed together with a shooting approach [14]–[16]. However, the local approximations yield only algebraic accuracy. This requires a fine grid and thus increased computational resources when high accuracy is in demand. In solving BVPs by using initial value solvers, on the other hand, a well-known drawback is that the associated IVP may not be stable [17].

In this work, we propose and implement a spectral collocation (pseudospectral) method for solving the model equations. Spectral methods are based on the global approximations and achieve exponential (spectral) accuracy when the solutions are sufficiently smooth [18]–[20]. Under the proposed pseudospectral method, a global polynomial representation of the dependent variables in terms of Chebyshev polynomials is introduced into the model equations and the resulting residual is forced to vanish at the collocation points yielding a system of nonlinear algebraic equations. The collocation points are the Gauss–Lobatto–Chebyshev (GLC) quadrature points and form a grid for optimal and stable representation of the dependent variables. The representation is optimal in the sense that it allows the use of a coarser grid and therefore fewer computational resources. The stability of the representation, on the other hand, allows the evaluation of the solution anywhere in the computational domain by global polynomial interpolation.

Eventually, the model differential equations are reduced to a system of nonlinear algebraic equations which is subsequently solved using the conventional Newton method. The well-known criterion for the convergence of the Newton iterates is to start the iteration with a sufficiently close initial approximation [21]. The crude initial approximations such as straight lines through the boundary values may not be sufficient to produce convergence and hence more sophisticated approaches such as param-

Manuscript received December 28, 2007; revised June 28, 2008. First published May 02, 2009; current version published June 26, 2009.

H. I. Tarman is with the Department of Engineering Sciences, Middle East Technical University, Ankara 06531, Turkey (e-mail: tarman@metu.edu.tr).

H. Berberoğlu is with the Department of Physics, Pamukkale University, Denizli, Turkey. Currently, he is a post-doctorate student at the Department of Physics, Middle East Technical University, Ankara 06531, Turkey.

Digital Object Identifier 10.1109/JLT.2008.2007506

TABLE I
SIMULATION PARAMETERS [9]

| Stokes order | Frequency (THz) | Raman Gain ($\mathrm{W^{-1}km^{-1}}$) | Absorption ($\mathrm{km^{-1}}$) |
|---|---|---|---|
| 0(pump) | 281 | 2.576 | 0.143 |
| 1 | 268 | 2.455 | 0.118 |
| 2 | 255 | 2.114 | 0.0969 |
| 3 | 242 | 1.786 | 0.0852 |
| 4 | 228 | 1.474 | 0.0814 |
| 5 | 215 | 1.181 | 0.194 |
| 6 | 202 | 0.912 | 0.0436 |

eter continuation techniques need to be employed [11]. In the absence of a Rayleigh backscattering term, the availability of a good initial approximation is especially crucial in order to stay clear of the trivial solution where the pump is depleted only by linear attenuation without generating any Stokes light. For this purpose, we present a new approach for constructing an initial approximate solution based on an integral of the dependent variables. It is tested in various numerical experiments that the approach produces robust initial approximations. Moreover, this approach allows highly accurate evaluation of certain integral quantities providing a way of assessing the degree of accuracy in the numerical results. The proposed Chebyshev pseudospectral method in combination with the Newton method and the initial approximation algorithm will be referred to as pseudospectral algorithm.

## II. THEORETICAL MODEL

The numerical algorithm presented here is developed for the simulation of the steady-state FRLs. The evolution of the powers in a Raman gain fiber is governed by the following system of coupled nonlinear ordinary differential equations [9]:

$$\begin{aligned}
\pm\frac{dP_0^{\pm}}{dz} &= -\alpha_0 P_0^{\pm} - g_0 P_0^{\pm}(P_1^{+} + P_1^{-}) \\
\pm\frac{dP_j^{\pm}}{dz} &= -\alpha_j P_j^{\pm} - g_j P_j^{\pm}(P_{j+1}^{+} + P_{j+1}^{-}) \\
&\quad + g_j P_j^{\pm}(P_{j-1}^{+} + P_{j-1}^{-}) \\
\pm\frac{dP_n^{\pm}}{dz} &= -\alpha_n P_n^{\pm} + g_n P_n^{\pm}(P_{n-1}^{+} + P_{n-1}^{-})
\end{aligned} \tag{1}$$

where $P_0$ and $P_j$ represent the powers of the input pump light and the desired $j$th-order Stokes light for $j = 1, \ldots, n$, respectively. The superscript $+/-$ stands for the forward/backward propagating wave in the cavity. Here, $\alpha$ denotes the intrinsic fiber loss coefficient and $g$ the Raman gain between adjacent waves. The boundary conditions for the forward pumping configuration are given by the input pump power $P_{\mathrm{in}}$ and by the Bragg gratings which are located at points $z = 0$ and $z = L$

$$\begin{aligned}
P_0^{+}(0) &= P_{\mathrm{in}} \\
P_i^{+}(0) &= R_i^{-} P_i^{-}(0) \\
P_j^{-}(L) &= R_j^{+} P_j^{+}(L)
\end{aligned} \tag{2}$$

for $i = 1, \ldots, n$ and $j = 0, \ldots, n$. Here, $R$ denotes the reflectivity coefficients of Bragg gratings with the positive and negative superscripts denoting the output side ($z = L$) and the input side ($z = 0$), respectively. $R_n^{+} = R_{\mathrm{OC}}$ is the reflectivity coefficient of the output coupler. $L$ is the length of the fiber cavity. For the sake of numerical demonstration, we ignore splicing and insert loss. We did not include the amplified spontaneous emission effect and Rayleigh backscattering.

It can be shown that the model equations possess the trivial solution

$$\begin{aligned}
P_0^{+}(z) &= P_{\mathrm{in}} \exp(-\alpha_0 z) \\
P_0^{-}(z) &= R_0^{+} P_{\mathrm{in}} \exp(\alpha_0 (z - 2L))
\end{aligned} \tag{3}$$

and $P_j^{\pm} = 0$ for $j \geq 1$. This is the case where the pump is depleted only by linear attenuation without generating any Stokes light. However, only the nontrivial (physical) solution shaped by the nonlinear interactions is of interest and it is characterized by $P_j^{\pm} > 0$ for $j = 0, 1, \ldots, n$.

As a numerical prototype, we consider a sixth-order cascaded Raman fiber laser with silica-based fiber in accordance with the simulation parameters used in [9] and listed in Table I.

## III. NUMERICAL FORMULATION

In order to present the numerical formulation, we consider the model BVP (1) in the following form:

$$\frac{d\mathbf{P}}{dz} = \mathbf{G}(\mathbf{P}) = [\mathbf{A} + \mathbf{Q}(\mathbf{P})]\mathbf{P} \tag{4}$$

subject to the boundary conditions

$$\mathbf{g}(\mathbf{P}(0), \mathbf{P}(L)) = \mathbf{C}^0 \mathbf{P}(0) + \mathbf{C}^L \mathbf{P}(L) = \mathbf{P}_{\mathrm{BC}} \tag{5}$$

where $\mathbf{G}, \mathbf{g}$, and $\mathbf{P}$ are N-vectors and $\mathbf{Q}(\mathbf{P}) = \mathrm{diag}(\mathbf{BP})$ is the diagonal matrix with the N-vector $\mathbf{BP}$ as its diagonal. The data of the problem are given in the block form by

$$\mathbf{A} = \begin{bmatrix} \mathbf{A}_0 & & & \\ & \mathbf{A}_1 & & \\ & & \ddots & \\ & & & \mathbf{A}_n \end{bmatrix}$$

$$\mathbf{B} = \begin{bmatrix} 0 & \mathbf{B}_0^{+} & & \\ \mathbf{B}_1^{-} & 0 & \ddots & \\ & \ddots & \ddots & \mathbf{B}_{n-1}^{+} \\ & & \mathbf{B}_n^{-} & 0 \end{bmatrix} \tag{6}$$

and by

$$\mathbf{C}^0 = \begin{bmatrix} \mathbf{C}_0^0 & & & \\ & \mathbf{C}_1^0 & & \\ & & \ddots & \\ & & & \mathbf{C}_n^0 \end{bmatrix}$$
$$\mathbf{C}^L = \begin{bmatrix} \mathbf{C}_0^L & & & \\ & \mathbf{C}_1^L & & \\ & & \ddots & \\ & & & \mathbf{C}_n^L \end{bmatrix} \tag{7}$$

with

$$\mathbf{B}_j^{\pm} = \pm g_j \mathbf{E} \tag{8}$$

and

$$\mathbf{A}_j = \begin{bmatrix} -\alpha_j & 0 \\ 0 & \alpha_j \end{bmatrix}, \quad \mathbf{E} = \begin{bmatrix} -1 & -1 \\ 1 & 1 \end{bmatrix}$$
$$\mathbf{C}_j^0 = \begin{bmatrix} 1 & -R_j^- \\ 0 & 0 \end{bmatrix}, \quad \mathbf{C}_j^L = \begin{bmatrix} 0 & 0 \\ -R_j^+ & 1 \end{bmatrix} \tag{9}$$

where $R_0^- = 0$ and $R_n^+ = R_{\mathrm{OC}}$. Here, we are assuming that the elements of the vector $\mathbf{P} = \mathbf{P}(z)$ stand for

$$\mathbf{P}(z) = [\, P_0^+ \quad P_0^- \quad \cdots \quad P_j^+ \quad P_j^- \quad \cdots \quad P_n^+ \quad P_n^- \,]^T \tag{10}$$

with $N = 2n + 2$. Thus, $\mathbf{P}_{\mathrm{BC}} = [\, P_{\mathrm{in}} \quad 0 \quad \cdots \quad 0 \,]^T$.

### A. Newton Formulation

The model two-point BVP (4) can be treated as a nonlinear system of equations

$$\mathbf{F}(\mathbf{P}) = \frac{d\mathbf{P}(z)}{dz} - \mathbf{G}(\mathbf{P}) = 0. \tag{11}$$

The most popular method for solving nonlinear equations is the Newton method. It is based on the repeated quasilinearization of the system around increasingly improved estimate of the solution. It leads to the iteration scheme

$$\mathbf{P}^{k+1}(z) = \mathbf{P}^k(z) + \mathbf{h}^k(z) \tag{12}$$

for $k = 0, 1, \ldots$ with linear equation

$$\left[\frac{d}{dz} - \frac{\partial \mathbf{G}(\mathbf{P}^k)}{\partial \mathbf{P}}\right] \mathbf{h}^k = -\left[\frac{d\mathbf{P}^k(z)}{dz} - \mathbf{G}(\mathbf{P}^k)\right] \tag{13}$$

to be solved for $\mathbf{h}^k(z)$ and subject to the homogeneous boundary conditions

$$\frac{\partial \mathbf{g}}{\partial \mathbf{a}} \mathbf{h}^k(0) + \frac{\partial \mathbf{g}}{\partial \mathbf{b}} \mathbf{h}^k(L) = 0 \tag{14}$$

assuming that the initial approximate solution $\mathbf{P}^0(z)$ satisfies the boundary conditions (5). Here, $\mathbf{a} = \mathbf{P}(0)$, $\mathbf{b} = \mathbf{P}(L)$ with $\partial \mathbf{g}/\partial \mathbf{a} = \mathbf{C}^0$ and $\partial \mathbf{g}/\partial \mathbf{b} = \mathbf{C}^L$, and

$$\mathbf{J}(\mathbf{P}) \equiv \frac{\partial \mathbf{G}(\mathbf{P})}{\partial \mathbf{P}} = \mathbf{A} + \mathrm{diag}(\mathbf{B}\mathbf{P}) + \mathrm{diag}(\mathbf{P})\mathbf{B}. \tag{15}$$



Fig. 1. The distribution of GLC grid points in $[-1, 1]$.

### B. Pseudospectral Formulation

The final step of the formulation is the introduction of a pseudospectral discretization so that the dependent variables and the differential operator are approximated over the grid $\{x_j\}_{j=0}^M$. In this paper, we have used GLC points as the underlying grid

$$x_j = -\cos \pi j/M, \quad \text{for } j = 0, 1, \ldots, M. \tag{16}$$

These points are associated with Gauss quadrature [19]. For BVPs GLC appears as the natural choice as it contains the boundary nodes $x_0 = -1$ and $x_M = 1$ and exhibits the grid distribution that is denser near the boundaries as shown in Fig. 1. The natural interval $[-1, 1]$ in which GLC points are located may be adapted to the interval $[0, L]$ at hand by a linear transformation $z(x) = (L)/(2)(x + 1)$.

In Chebyshev pseudospectral method, we seek polynomial solutions for a variable $P(z)$ in the modal form

$$P(z(x)) = \sum_{j=0}^{M} a_j T_j(x) \tag{17}$$

where $T_j(x) = \cos(j \arccos(x))$ are the Chebyshev polynomials and $a_j$ are discrete expansion coefficients [19] or, equivalently, in the nodal form

$$P(z(x)) = \sum_{j=0}^{M} P(z_j) L_j(x) \tag{18}$$

where $z_j = z(x_j)$ and $L_j(x)$ is the $j$th-order Lagrange polynomial based on the grid $\{x_j\}_{j=0}^M$ satisfying the cardinality property $L_j(x_i) = \delta_{ij}$. The later form is more convenient in approximating the derivative of $P(z)$ at any point $z_i$ by differentiating the Lagrange polynomial

$$\frac{d}{dz} P(z_i) = \frac{2}{L} \sum_{j=0}^{M} P(z_j) L_j'(x_i)$$
$$= \frac{2}{L} \sum_{j=0}^{M} P(z_j) D_{ij} \tag{19}$$

where $D$ is the differentiation matrix. The reader is referred to [18] and [22] for Matlab implementation.

Before discretizing the model equations, we introduce the following notation for the discretized form of the variable $\mathbf{P}$ as

$$\mathbf{P}_j = \begin{bmatrix} P_1(z_j) \\ P_2(z_j) \\ \vdots \\ P_N(z_j) \end{bmatrix} \tag{20}$$

with

$$\{\mathbf{P}_j\} = \begin{bmatrix} P_1(z_0) & P_1(z_1) & \cdots & P_1(z_M) \\ P_2(z_0) & P_2(z_1) & \cdots & P_2(z_M) \\ \vdots & \vdots & \ddots & \vdots \\ P_N(z_0) & P_N(z_1) & \cdots & P_N(z_M) \end{bmatrix} \tag{21}$$

and for the vectorization operation as

$$\text{vec}(\mathbf{h}) = [h_1(z_0)h_2(z_0)\cdots h_N(z_0) \times h_1(z_1)\cdots h_N(z_M)]^T. \tag{22}$$

Now introducing the pseudospectral discretization to (13) yields the matrix form

$$\left[\frac{2}{L}\mathbf{D}\otimes\mathbf{I}_N - \text{diag}(\mathbf{J}(\mathbf{P}_j^k))\right]\text{vec}(\mathbf{h}^k) = -\text{vec}\left(\frac{2}{L}\{\mathbf{P}_j^k\}\mathbf{D}^T - \{\mathbf{G}(\mathbf{P}_j^k)\}\right) \tag{23}$$

where $\mathbf{I}_N$ is the $N \times N$ identity matrix, $\otimes$ is the Kronecker product [23], $\{\mathbf{G}(\mathbf{P}_j)\} = [\mathbf{G}(\mathbf{P}_0)\mathbf{G}(\mathbf{P}_1)\cdots\mathbf{G}(\mathbf{P}_M)]$, and

$$\text{diag}\,(\mathbf{J}(\mathbf{P}_j)) = \begin{bmatrix} \mathbf{J}(\mathbf{P}_0) & & & \\ & \mathbf{J}(\mathbf{P}_1) & & \\ & & \ddots & \\ & & & \mathbf{J}(\mathbf{P}_M) \end{bmatrix}. \tag{24}$$

The resulting matrix form (23) is modified to accommodate the boundary conditions as follows:

$$\begin{bmatrix} \mathbf{C}_0 & \mathbf{0} & \mathbf{C}_L \\ \vdots & \vdots & \vdots \\ \vdots & \vdots & \vdots \end{bmatrix}\text{vec}(\mathbf{h}^k) = \begin{bmatrix} \mathbf{0} \\ \vdots \\ \vdots \end{bmatrix}. \tag{25}$$

### C. Initial Approximation Algorithm

The local convergence theory for the Newton method requires that the initial approximate solution $\mathbf{P}^0(z)$ be near the solution [21]. This can be achieved by constructing an initial approximation that carries as much property of the actual solution as possible. Our strategy consists of solving the system (1) for an integral of the solution and then constructing an assumed exponential form of the solution that has the same integral values. It turns out that some of these integrals are the solution to a linear system and can be computed with high accuracy, thus providing a way of assessing the accuracy of the computed solution.

In order to facilitate the construction of such an initial approximation, the coupled system of differential equations (1) are integrated with respect to $z$ from 0 to $L$ to get the system of equations

$$\begin{aligned} \pm U_0^{\pm} &= -\alpha_0 - g_0 S_1 \\ \pm U_j^{\pm} &= -\alpha_j - g_j S_{j+1} + g_j S_{j-1} \\ \pm U_n^{\pm} &= -\alpha_n + g_n S_{n-1} \end{aligned} \tag{26}$$

where

$$S_j = \frac{1}{L}\int_0^L (P_j^+ + P_j^-)\,dz \tag{27}$$

and

$$U_j^{\pm} = \frac{1}{L}\ln\frac{P_j^{\pm}(L)}{P_j^{\pm}(0)}. \tag{28}$$

By using the coupled boundary conditions (2) and the known relation $P_j^+P_j^- = c_j$, where $c_j$ is a constant, one can show that

$$U_j^- = -U_j^+ = \frac{1}{2L}\ln(R_j^+R_j^-), \quad j \geq 1. \tag{29}$$

It should be noted that in the case of the assumed exponential solution

$$P_j^{\pm}(z) = P_j^{\pm}(0)\exp(\mp\beta_j z) \tag{30}$$

we have

$$U_j^- = -U_j^+ = \beta_j \tag{31}$$

and

$$S_j = \frac{P_j^+(0)}{\beta_j L}[1-\exp(-\beta_j L)] \times [1 + R_j^+\exp(-\beta_j L)] \tag{32}$$

together with

$$P_j^-(0) = P_j^+(0)R_j^+\exp(-2\beta_j L). \tag{33}$$

It is convenient to consider the problem separately for the cases of $n$ odd and $n$ even.

For $n$ odd, we define

$$\mathbf{S}_e = [\,S_0 \quad S_2 \quad \cdots \quad S_{n-1}\,]^T \tag{34}$$

and

$$\mathbf{S}_o = [\,S_1 \quad S_3 \quad \cdots \quad S_n\,]^T. \tag{35}$$

We then have

$$\begin{bmatrix} g_1 & -g_1 & & & \\ & g_3 & -g_3 & & \\ & & \cdots & \cdots & \\ & & & g_{n-2} & -g_{n-2} \\ & & & & g_n \end{bmatrix}\mathbf{S}_e = \begin{bmatrix} U_1^+ + \alpha_1 \\ U_3^+ + \alpha_3 \\ \vdots \\ U_{n-2}^+ + \alpha_{n-2} \\ U_n^+ + \alpha_n \end{bmatrix} \tag{36}$$

and

$$\begin{bmatrix} -g_0 & & & & \\ g_2 & -g_2 & & & \\ & \cdots & \cdots & & \\ & & g_{n-3} & -g_{n-3} & \\ & & & g_{n-1} & -g_{n-1} \end{bmatrix}\mathbf{S}_o$$

$$= \begin{bmatrix} U_0^+ + \alpha_0 \\ U_2^+ + \alpha_2 \\ \vdots \\ U_{n-3}^+ + \alpha_{n-3} \\ U_{n-1}^+ + \alpha_{n-1} \end{bmatrix}. \tag{37}$$

We propose the following scheme:

1) Solve the linear system (36) for the values of $\mathbf{S}_e$.
2) Assume $P_0^{\pm}(z) = P_0^{\pm}(0)\exp(\mp\beta_0 z)$ with $P_0^+(0) = P_{\text{in}}$. This gives

$$S_0 = \frac{P_{\text{in}}}{\beta_0 L}[1 - \exp(-\beta_0 L)][1 + R_0^+ \exp(-\beta_0 L)] \tag{38}$$

to be solved for $\beta_0$, and thus $U_0^+ = -\beta_0$.
3) Now, solve the linear system (37) for $\mathbf{S}_o$.

For $n$ even, we define

$$\mathbf{S}_e = [\, S_2 \quad S_4 \quad \cdots \quad S_n \,]^T \tag{39}$$

and

$$\mathbf{S}_o = [\, S_1 \quad S_3 \quad \cdots \quad S_{n-1} \,]^T. \tag{40}$$

We then have

$$\begin{bmatrix} g_2 & -g_2 & & & & \\ & g_4 & -g_4 & & & \\ & & \cdots & \cdots & & \\ & & & g_{n-2} & -g_{n-2} & \\ & & & & g_n & \end{bmatrix} \mathbf{S}_o = \begin{bmatrix} U_2^+ + \alpha_2 \\ U_4^+ + \alpha_4 \\ \vdots \\ U_{n-2}^+ + \alpha_{n-2} \\ U_n^+ + \alpha_n \end{bmatrix} \tag{41}$$

and

$$\begin{bmatrix} -g_1 & & & & & \\ g_3 & -g_3 & & & & \\ & \cdots & \cdots & & & \\ & & g_{n-3} & -g_{n-3} & & \\ & & & g_{n-1} & -g_{n-1} & \end{bmatrix} \mathbf{S}_e = \begin{bmatrix} U_1^+ + \alpha_1 - g_0 S_0 \\ U_3^+ + \alpha_3 \\ \vdots \\ U_{n-3}^+ + \alpha_{n-3} \\ U_{n-1}^+ + \alpha_{n-1} \end{bmatrix}. \tag{42}$$

We now propose the following scheme:

1) Solve the linear system (41) for the values of $\mathbf{S}_o$.
2) Solve $-\alpha_0 - g_0 S_1 = U_0^+$ for $U_0^+$. This gives $\beta_0 = -U_0^+$ and subsequently

$$S_0 = \frac{P_{\text{in}}}{\beta_0 L}[1 - \exp(-\beta_0 L)][1 + R_0^+ \exp(-\beta_0 L)] \tag{43}$$

when the form of the solution is assumed as $P_0^{\pm}(z) = P_0^{\pm}(0)\exp(\mp\beta_0 z)$.
3) Now, solve the linear system (42) for $\mathbf{S}_e$.

The approximation for $P_j^{\pm}(z)$ is constructed in the exponential form (30) with $\beta_j = -U_j^+$ and $P_j^{\pm}(0)$ obtained from (32) and (33) using the computed $S_j$ values.

## IV. Results and Discussion

The performance of the initial approximation for $P_j^{\pm}(z)$ is numerically tested under various problem parameters such as, $P_{\text{in}}$, $R$, $R_{\text{OC}}$, $L, M$, $n$ using the data in Table I. The above outlined procedure for generating initial approximate solution is observed to produce robust estimates facilitating fast convergence of subsequent Newton iterations. Throughout the computations, the convergence of the Newton iterates is monitored using the relative error estimate satisfying

$$\frac{\|\mathbf{h}^k\|}{\|\mathbf{P}^k\|} \leq \text{TOL}. \tag{44}$$

It is known that for superlinearly convergent methods the theory supports the approach of exploiting the fast convergence to estimate the error in terms of the step size $\|\mathbf{h}^k\| = \|\mathbf{P}^k - \mathbf{P}^{k-1}\|$, hence the use of the step size as a basis for termination [21].

A validation of the computed solution is performed in comparison to the analytic solution reported in [9] obtained from the coupled (1) using some approximations. The approximation procedure is detailed in [9] and shown to lead to a satisfactory analytic solution for high reflectivities. We have solved the model system (1) using the proposed pseudospectral algorithm for the case with 96.7% reflectivity mirrors and 10% output mirror. The cavity length is taken as 150 m and the injected pump power 6 W. The resulting computed wave power profiles (curves) are shown in Fig. 2(b) in comparison to the analytic solution (symbols) that is also presented in Fig. 2 of [9] for the same parameter values. The comparison yields a relative error of around 1% of the computed solution. This is in agreement with the results reported in [9] where a standard shooting method with an adaptive step-size Runge–Kutta integrator is used to obtain the computed solution. The patterns appearing in Fig. 2(b) for the two Stokes light adjacent to the pump and the $n$th Stokes lights are of fundamental standing wave type as pointed out in [11]. The converged solution in Fig. 2(b) is obtained starting from the generated initial approximation shown in Fig. 2(a). It took only four Newton iterations to satisfy the convergence criteria $\text{TOL} = 10^{-14}$ in maximum norm. This shows the quality of the initial estimate in that the subsequent iterations readily enter the zone of quadratic speed of convergence where the number of significant digits in the iterates roughly doubles with each iteration.

In order to demonstrate the optimal and stable global representation provided by the pseudospectral method based on the GLC grid, we have compared against the numerical solution obtained using a widely available collocation BVP solver [13]. It uses a local cubic polynomial approximation within each subinterval of the mesh and collocates the differential equation at both ends and the midpoint of each subinterval. It is based on residual control and provides the numerical solution over an adaptive grid whose size is determined by the user supplied absolute $\tau_a$ and relative tolerances $\tau_r$ on the residual. The BVP solver is used to solve the system (1) for successively reduced tolerance values $\tau_a = \tau_r = \tau$ and the size of the resulting grid is recorded for the subsequent comparison. In using the BVP solver, we have supplied the exact Jacobian and the initial approximation constructed by our algorithm.

In Fig. 3, the comparison is presented against the values of $\mathbf{S}_o$ (for the even case $n = 6$) obtained by solving the linear

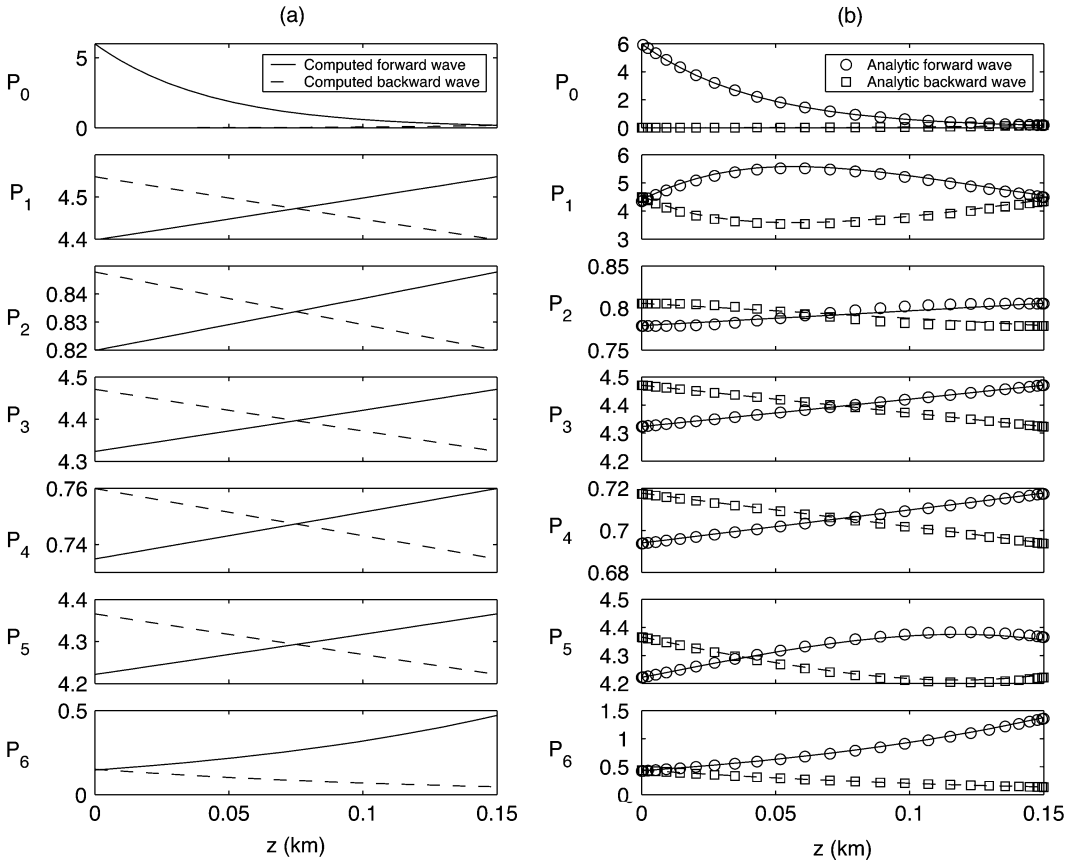


Fig. 2. (a) The initial approximate solution and (b) the comparison between computed and analytic [9] Stokes powers inside the cavity for the data in Table I.

system (41) and deemed to be highly accurate. The computed $\tilde{\mathbf{S}}_o$ values corresponding to the numerical methods are obtained by numerically evaluating the integral

$$S_j \approx \frac{1}{L}\sum_{q=0}^{Q}\omega_q(P_j^+(\xi_q)+P_j^-(\xi_q)) = \tilde{S}_j \qquad (45)$$

using Legendre Gauss quadrature formula with quadrature weights $\omega_q$ and the computed $P_j^{\pm}$ values interpolated at the quadrature nodes $\xi_q$. It should be noted that the quadrature formula is exact for polynomials of degree $\leq 2Q+1$ [19]. The proposed pseudospectral method has the added advantage at this point in providing a global polynomial representation of the solution as well as enabling the evaluation of the $P_j^{\pm}$ values at the nongrid quadrature nodes $\xi_q$ by stable global polynomial interpolation. The smallest size $Q$ of the quadrature to produce the most attainable accuracy for the level of accuracy carried by the computed solution can be determined. However, we simply use the size of the grid underlying the computed solution as $Q$.

The exponential (spectral) accuracy as well as the optimal representation achieved under the pseudospectral method is clearly visible in Fig. 3 (solid squares) producing results in near-machine precision with a resolution of just $M \approx 20$. The error decreases algebraically like $O(M^{-4})$ (hollow squares) for the case of the BVP solver [13]. In generating the corresponding error curve the tolerance $\tau$ is gradually varied in the range $10^{-4}$ to $10^{-8}$ and the resulting grid sizes are recorded. This convergence rate is typical of local methods, requiring high-order discretization for high accuracy and thus resulting in large systems. Another comparison is performed directly between $P_j^{\pm}$ values computed using the proposed pseudospectral method with varying resolution parameter $M$ and a reference solution computed using the BVP solver by setting $\tau = 10^{-10}$ resulting in a mesh of size 784. The error exhibits similar exponential decay trend (hollow circles) with

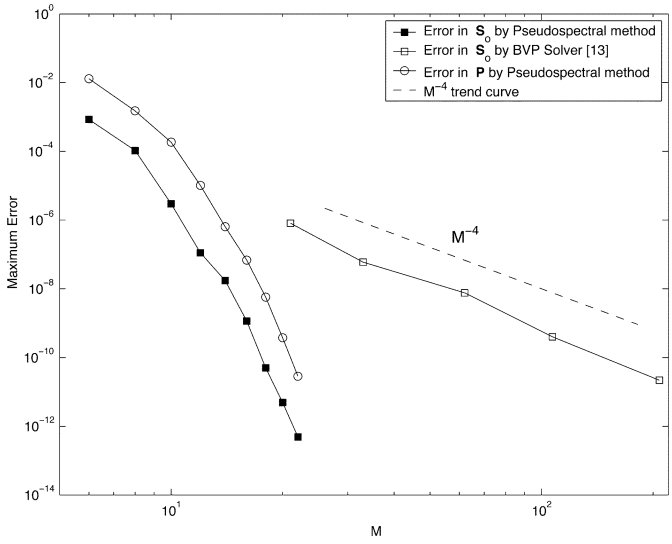


Fig. 3. The maximum error $\|\mathbf{S}_o - \tilde{\mathbf{S}}_o\|_\infty$ computed using the solution obtained by the pseudospectral method and by the BVP solver [13]. Also shown is the maximum error in the solution $P_j^{\pm}$ computed using the pseudospectral method in comparison to a reference solution obtained by the BVP solver.

some orders of magnitude higher in comparison to the error in the integral values $S_j$ (solid squares) in Fig. 3. This shows the high accuracy in the integral values computed by directly solving the linear system (41), which resulted as a byproduct of our initial approximation algorithm.

In the computations, the tolerance on the Newton step size in the pseudospectral algorithm is fixed at $\mathrm{TOL} = 10^{-14}$ that is close to the machine accuracy in order to attain the maximum possible accuracy for given $M$. It should be noted that even though the Newton iterates satisfy the stopping criteria set by the fixed tolerance, the estimated error (solid squares) in the resulting solution varies with varying resolution in Fig. 3. This is because the solution in the proposed pseudospectral formulation is searched within the polynomial space of degree $\leq M$. Thus, the size of the resolution parameter $M$ restricts the size of the solution space and in turn restricts the attainable accuracy in the resulting solution.

## V. Conclusion

In this study, the focus was mainly on the implementation of a pseudospectral method for solving FRL model equations. A detailed formulation of the algorithm was presented using the modular and compact language of matrices. The reader may easily implement the pseudospectral procedure by the Matlab routines provided in [18] and [22]. As demonstrated by the numerical experiments, the proposed pseudospectral method used much coarser grid compared to the local method for given accuracy and reached to the goal of the efficient and robust numerical technique for the model equations. This is a typical character of spectral methods that belong to the class of high-order computational methods. The pseudospectral method implemented is just a particular example of the spectral methods, and there are other types to explore along the way to increase the efficiency of the solver. It is hoped that this work will generate an interest and capture the attention of the optics community toward a wider use of spectral methods in computational optics.

In the process a procedure was developed to construct a good quality initial approximation for the subsequent Newton iteration. The natural appearance of the need for separately treating the cases of even and odd number of Stokes waves in the construction procedure is shown in [9] to have fundamental effects on the laser behavior. As a result of the efforts to construct an initial approximate solution that carries as much property of the actual solution, this procedure is closely linked to the character of the problem. It may further be developed in order to construct problem specific numerical techniques for highly efficient solvers by working out the correspondence between the pointwise values of the dependent variable and its integral.

Other issues such as efficient solution techniques for the Newton iterates are subject for another study. As the size of the system increases, the direct method of solution loses its efficiency and should be replaced by iterative methods. Coupling the Newton iteration (outer iteration) with a popular Krylov subspace based iterative method of solving Newton linear equations (inner iterations) results in an efficient solution technique referred to as Newton–Krylov iterations [21].

## References


[1] R. H. Stolen and E. P. Ippen, "Raman gain in glass optical waveguides," *Appl. Phys. Lett.*, vol. 22, pp. 276–278, 1973.

[2] G. Agrawal, *Nonlinear Fiber Optics*. New York: Academic, 2001.

[3] J. AuYeung and A. Yariv, "Theory of CW Raman oscillation in optical fibers," *J. Opt. Soc. Amer.*, vol. 69, pp. 803–807, 1979.

[4] M. Rini, I. Cristiani, V. Degiorgio, A. S. Kurkov, and V. M. Paramonov, "Experimental and numerical optimization of a fiber Raman laser," *Opt. Commun.*, vol. 203, pp. 139–144, 2002.

[5] S. Cierullies, M. Krause, H. Renner, and E. Brinkmeyer, "Experimental and numerical study of the switching dynamics of Raman fiber lasers," *Appl. Phys. B, Photophys. Laser Chem.*, vol. 80, pp. 177–183, 2005.

[6] M. Rini, I. Cristiani, and V. Degiorgio, "Numerical modelling optimization of cascaded CW Raman fiber lasers," *IEEE J. Quantum Electon.*, vol. 36, no. 10, pp. 1117–1122, Oct. 2000.

[7] B. Burgoyne, N. Godbout, and S. Lacroix, "Theoretical analysis of $n$th-order cascaded continuous-wave Raman fiber lasers. II. Optimization and design rules," *J. Opt. Soc. Amer. B, Opt. Phys.*, vol. 22, no. 4, pp. 772–76, Apr. 2005.

[8] I. A. Bufetov and E. M. Dianov, "A simple analytic model of a CW multicascade fibre Raman laser," *Quantum Electron.*, vol. 30, no. 10, pp. 873–877, Oct. 2000.

[9] B. Burgoyne, N. Godbout, and S. Lacroix, "Theoretical analysis of $n$th-order cascaded continuous-wave Raman fiber lasers. I. Model and resolution," *J. Opt. Soc. Amer. B, Opt. Phys.*, vol. 22, no. 4, pp. 764–71, Apr. 2005.

[10] C. Huang, Z. Cai, C. Ye, and H. Xu, "Explicit solution for Raman fiber laser using Lambert $W$ function," *Opt. Exp.*, vol. 15, no. 8, pp. 4671–4676, 2007.

[11] S. D. Jackson and P. H. Muir, "Theory and numerical simulation of $n$th-order cascaded Raman fiber lasers," *J. Opt. Soc. Amer. B, Opt. Phys.*, vol. 18, no. 9, pp. 1297–1305, Sep. 2001.

[12] U. Ascher, J. Christiansen, and R. D. Russell, "Collocation software for boundary-value ODEs," *ACM Trans. Math. Softw.*, vol. 7, no. 1, pp. 209–222, Jun. 1981.

[13] L. F. Shampine, M. W. Reichelt, and J. Kierzenka, "Solving BVPs for ordinary differential equations in MATLAB with bvp4c," Mathworks Inc., Natick, MA., 2000 [Online]. Available: http://www.mathworks.com/bvp_tutorial

[14] M. Krause and H. Renner, "Theory and design of double-cavity Raman fiber lasers," *J. Lightw. Technol.*, vol. 23, no. 8, pp. 2474–2483, Aug. 2005.

[15] F. Leplingard, C. Martinelli, S. Borne, L. Lorcy, D. Bayart, F. Castella, P. Chartier, and E. Faou, "Modelling of multiwavelength Raman fiber lasers using a new and fast algorithm," *Photon. Technol. Lett.*, vol. 16, no. 12, pp. 2601–2603, Dec. 2004.

[16] H. Kaidi, Z. Xiaojun, Q. Zujun, W. Haocheng, and Z. Zili, "A novel fast numerical algorithm for cascaded Raman fiber laser using the analytic approximate solution," *Opt. Commun.*, vol. 271, pp. 257–262, 2007.

[17] U. M. Ascher and L. R. Petzold, *Computer Methods for Ordinary Differential Equations and Differential-Algebraic Equations*. Philadelphia, PA: SIAM, 1998.

[18] L. N. Trefethen, *Spectral Methods in Matlab*. Philadelphia, PA: SIAM, 2000.

[19] J. S. Hesthaven, S. Gottlieb, and D. Gottlieb, *Spectral Methods for Time-Dependent Problems*. Cambridge, U.K.: Cambridge Univ. Press, 2007.

[20] J. P. Boyd, *Chebyshev and Fourier Spectral Methods*. New York: Dover, 2000.

[21] C. T. Kelley, *Solving Nonlinear Equations with Newton's Method, in Fundamentals of Algorithms*. Philadelphia, PA: SIAM, 2003.

[22] J. A. C. Weideman and S. C. Reddy, "A MATLAB differentiation matrix suite," *ACM Trans. Math. Softw.*, vol. 26, pp. 465–519, 2000.

[23] A. Graham, *Kronecker Products and Matrix Calculus with Applications*. New York: Ellis Horwood Ltd., 2003.



**Hakan I. Tarman** was born in Izmir, Turkey. He received the B.S. degrees both in mechanical engineering and mathematics, the M.S. degree in mechanical engineering, and the Ph.D. degree in applied mathematics from Brown University, Providence, Rhode Island, USA, in 1982, 1984, and 1989, respectively.

He is currently a Professor at the Engineering Sciences Department, Middle East Technical University, Ankara, Turkey. His research interests include spectral methods and computational mechanics.

**Halil Berberoğlu** was born in Denizli, Turkey. He received the B.S. degree in engineering physics, the M.S. degree in physics from Lehigh University, Bethlehem, PA, USA, and the Ph.D. degree in physics from Middle East Technical University (METU), Ankara, Turkey, in 1992, 1996, and 2007, respectively.

He is currently a post-doctoral researcher at METU. His research interests include fiber Raman lasers, amplifiers, and THz spectroscopy.